Molecular Pharmacology Fast Forward. Published on March 31, 2015 as DOI: 10.1124/mol.114.097477
This article has not been copyedited and formatted. The final version may differ from this version.

TITLE PAGE

Dual Targeting of the Androgen Receptor and Hypoxia-inducible Factor 1α Pathways Synergistically Inhibits Castration-Resistant Prostate Cancer Cells

Elena V. Fernandez, Kelie M. Reece, Ariel M. Ley, Sarah M. Troutman, Tristan M. Sissung, Douglas K. Price, Cindy H. Chau, and William D. Figg

Genitourinary Malignancies Branch, Center for Cancer Research, National Cancer Institute, Bethesda, MD (E.V.F., K.M.R., A.M.L., S.M.T., T.S., D.K.P., C.H.C., W.D.F.)

Molecular Pharmacology Fast Forward. Published on March 31, 2015 as DOI: 10.1124/mol.114.097477
This article has not been copyedited and formatted. The final version may differ from this version.

RUNNING TITLE PAGE

Running Title: Synergistic Targeting of HIF-1α and AR in CRPC

Corresponding author:
William D. Figg
Bldg 10/Room 5A01
9000 Rockville Pike
Bethesda, MD 20892
Tel: 301-402-3623/Fax: 301-402-8606
figgw@helix.nih.gov

Number of text pages: 12
Number of tables: 0
Number of figures: 5 and 3 supplementary figures
Number of references: 25
Number of words in the abstract: 236
Number of words in the introduction: 518
Number of words in the discussion: 719

List of non-standard abbreviations: AR, androgen receptor; CRPC, castrate-resistant prostate cancer; $CoCl_{2,}$cobalt chloride; DHT, dihydrotestosterone; ENZ, enzalutamide; FBS, fetal bovine serum; HIF-1α, hypoxia-inducible factor-1 alpha; VEGF, vascular endothelial growth factor

Version date: 03-30-15

Molecular Pharmacology Fast Forward. Published on March 31, 2015 as DOI: 10.1124/mol.114.097477
This article has not been copyedited and formatted. The final version may differ from this version.

Abstract

Background: Enzalutamide is a potent second-generation androgen receptor (AR) antagonist with activity in metastatic castrate-resistant prostate cancer (CRPC). While enzalutamide is initially effective, disease progression inevitably ensues with the emergence of resistance. Intratumoral hypoxia is also associated with CRPC progression and treatment resistance. Given that both AR and hypoxia inducible factor 1-alpha (HIF-1α) are key regulators of these processes, dual targeting of both signaling axis represents an attractive therapeutic approach. **Methods:** Crosstalk of the AR and HIF-1α signaling pathways were examined in prostate cancer cell lines (LNCaP, 22Rv1) with assays measuring the effect of androgen and hypoxia on AR-dependent and hypoxia-inducible gene transcription, protein expression, cell proliferation, and apoptosis. HIF-1α inhibition was achieved by siRNA silencing HIF-1α or via chetomin, a disruptor of HIF-1α-p300 interactions. **Results:** In prostate cancer cells, the gene expression of AR targets (*KLK3, FKBP5, TMPRSS2*) was repressed by HIF-signaling; conversely, specific HIF-1α target expression was induced by DHT-mediated AR signaling. Treatment of CRPC cells with enzalutamide or HIF-1α inhibition attenuated AR-regulated and HIF-1α-mediated gene transcription. The combination of enzalutamide and HIF-1α inhibition was more effective than either treatment alone. Similarly, the combination also reduced VEGF protein levels. HIF-1α siRNA synergistically enhanced the inhibitory effect of enzalutamide on cell growth in LNCaP and enzalutamide-resistant 22Rv1 cells via increased enzalutamide-induced apoptosis. **Conclusions:** The combination of enzalutamide with HIF-1α inhibition resulted in synergistic inhibition of AR-dependent and gene-specific HIF-dependent expression and prostate cancer cell growth.

Molecular Pharmacology Fast Forward. Published on March 31, 2015 as DOI: 10.1124/mol.114.097477
This article has not been copyedited and formatted. The final version may differ from this version.

Introduction

The androgen receptor (AR), a member of the nuclear hormone receptor superfamily of proteins, is the transcription factor responsible for mediating the effects of androgens on target tissues. AR plays a critical role in the development and progression of prostate cancer. Mechanisms that underlie the transition from hormone-dependent prostate cancer to that of castration-resistance involve regulation at the AR level (Chen, Welsbie et al., 2004; Debes and Tindall, 2004). Despite androgen deprivation therapy, low levels of circulating androgens persist (Pienta and Bradley, 2006), and the AR can become transactivated in this low-androgen environment through various pathways and genetic aberrations involving molecular alterations to the receptor that lead to castration-resistance (Scher and Sawyers, 2005).

Therapy targeting persistent AR-mediated signaling led to the development of enzalatumide (MDV3100), a small-molecule, pure AR antagonist, second generation antiandrogen that improves upon the effects of current first generation antiandrogens (e.g. bicalutamide). The drug was selected as a result of its activity in CRPC models of AR overexpression, in which it showed selective, potent affinity for AR while being devoid of any agonist AR activity compared to bicalutamide (Tran, Ouk et al., 2009). Preclinical studies have shown that enzalutamide effectively inhibits AR nuclear translocation and DNA binding to androgen response elements, induces apoptotic effects on prostate cancer tumors, and prevents co-activator recruitment. Although enzalutamide has provided benefit to many, not all patients respond to therapy, and among those who do, the duration of response is often limited with the emergence of resistance (Nelson and Yegnasubramanian, 2013).

Molecular Pharmacology Fast Forward. Published on March 31, 2015 as DOI: 10.1124/mol.114.097477
This article has not been copyedited and formatted. The final version may differ from this version.

Androgen deprivation as a result of castration results in hypoxia in prostate cancer cells, (Halin, Hammarsten et al., 2007; Shabsigh, Ghafar et al., 2001) and subsequently enhances the transcriptional activity of AR. Thus, understanding the molecular mechanisms of aberrant AR signaling under hypoxic conditions is important. Intratumoral hypoxia is emerging as a common feature of prostate cancers that are associated with poor prognosis (Stewart, Ross et al., 2010). In prostate cancer progression, tumor cells acquire the ability to adapt to hypoxic environments by co-opting blood vessel formation while also migrating and invading toward vessels. The transcription factor hypoxia-inducible factor (HIF)-1α mediates key hypoxia-associated genes involved in angiogenesis, metabolism, survival, immunity and invasion (reviewed in (Greer, Metcalf et al. 2012; Semenza, 2010; Semenza, 2012).

The results of several studies (Horii, Suzuki et al., 2007; Mabjeesh, Willard et al., 2003; Mitani, Yamaji et al., 2011; Park, Kim et al., 2012) suggest that there is crosstalk between the AR and HIF-1α pathways that may converge on AR, HIF-1α, and β-catenin forming a ternary complex on androgen response elements of AR target genes (Mitani, Harada et al., 2012). Thus, HIF-1α might be involved in AR-mediated gene expression in prostate cancer and implicated in tumor growth and progression. Given that both AR and HIF-1α are key regulators of multiple cellular processes in prostate cancer, dual targeting of both axes represents an attractive therapeutic approach. The goal of our study was to evaluate the combination treatment of the novel AR antagonist enzalutamide with HIF inhibition in preclinical models of CRPC, and to define the molecular mechanism by which HIF-1α inhibition potentiates anti-AR therapy in CRPC.

Molecular Pharmacology Fast Forward. Published on March 31, 2015 as DOI: 10.1124/mol.114.097477
This article has not been copyedited and formatted. The final version may differ from this version.

MATERIALS AND METHODS

Cell culture

LNCaP and 22Rv1 (AR-positive human prostate cancer) cells (ATCC; Manassas, VA) were maintained in phenol red-free RPMI 1640 medium supplemented with 10% fetal bovine serum, 50 U/mL penicillin, and 50 mg/mL streptomycin unless otherwise indicated. For hypoxic conditions, cells were treated with hypoxia mimetic cobalt chloride (150 μM $CoCl_2$) (Sigma; St. Louis, MO).

Antibodies and reagents

Monoclonal HIF-1α antibody was purchased from BD Biosciences (San Diego, CA), and monoclonal Actin (C-2) antibody was purchased from Santa Cruz Biotechnology (Santa Cruz, CA). Alexa Fluor 680 goat anti-mouse IgG was obtained from Molecular Probes (Eugene, OR). Odyssey blocking buffer was from LICOR (Lincoln, NE). Dihydrotestosterone (DHT) was purchased from Steraloids, Inc. (Wilton, NH), Chetomin was purchased from Sigma, and enzalutamide was purchased from Selleck Chemicals (Houston, TX). The ARE3-TK-luc plasmid was kindly provided by Dr. Nima Sharifi (Sharifi, Hurt et al. 2008). The pRL-TK control and HRE-luc (pGL4.42) plasmids were obtained from Promega (Fitchburg, WI).

siRNA Transfection

Specific knockdown was achieved using siRNAs against HIF-1α (S104249308, Qiagen; Valencia, CA) or Allstars negative control siRNA (1027281, Qiagen). 22Rv1 or LNCaP cells were transiently transfected with control or HIF-1α siRNA at 20 nM using

Molecular Pharmacology Fast Forward. Published on March 31, 2015 as DOI: 10.1124/mol.114.097477
This article has not been copyedited and formatted. The final version may differ from this version.

Lipofectamine 2000 (Invitrogen; Carlsbad, CA) according to the manufacturer's instructions for 24 h or 48 h.

Western blot analysis

Cells were lysed with 400 μL ice-cold lysis buffer (2.5% (v/v) Tris pH 8, 3% (v/v) 5 M NaCl, 0.4% (v/v) 0.5 M EDTA, 1% (v/v) Triton, and complete protease inhibitors). After 30 min of incubation on ice, cell lysates were centrifuged at 7500 rpm for 10 min. Supernatants were collected and total protein concentration was determined using the BCA assay (Thermo Scientific; Waltham, MA) according to the manufacturers protocol. Cell lysates were subjected to SDS-PAGE and analyzed by Western blotting with anti-HIF-1α monoclonal antibody or anti-actin monoclonal antibody. Primary antibody was immunoreacted with fluorophore-conjugated goat anti-mouse IgG. Bound antibodies were visualized, and densitometry was completed via the Odyssey Infrared Imaging System and Odyssey software.

Cell viability assays

LNCaP cells were seeded in 96-well plates in 100 μL 10% FBS supplemented phenol red-free RPMI 1640 medium. After overnight incubation at 37°C, cells were transiently transfected with siRNA. Forty-eight hours after siRNA transfection, cells were treated with charcoal-stripped phenol red-free RPMI 1640 containing 150 μM $CoCl_2$, and 1 nM DHT with or without 1 μM enzalutamide (Day 0). Cell viability was measured on days 0, 1, 2, 3, and 4 using the Cell Counting-Kit 8 cell viability assay according to the manufacturer's instructions (Dojindo; Rockville, MD), and absorbance was read at 450

Molecular Pharmacology Fast Forward. Published on March 31, 2015 as DOI: 10.1124/mol.114.097477
This article has not been copyedited and formatted. The final version may differ from this version.

nm using a SpectraMax M2 fluorescence plate reader (Molecular Devices; Sunnyvale, CA).

Semi-quantitative real time-PCR (qPCR)

LNCaP cells were plated at a density of 400,000 cells per well in a 6-well dish in phenol red-free RPMI 1640 charcoal-stripped media for 48 h, and then treated for 18 h with combinations of DHT, chetomin, and enzalutamide in normoxia or hypoxia (150 μM $CoCl_2$). Treatments were completed in duplicate, and total RNA extraction was performed using the QIAshredder and RNAeasy mini kit (Qiagen) according to the manufacturer's protocol. RNA concentration was determined using a NanoDrop® spectrophotometer (Molecular Devices). Purified RNA (0.24–0.32 □g) from LNCaP cells was reverse transcribed per 30 μl cDNA synthesis reaction using The Superscript III First-Strand Synthesis System for RT-PCR (Invitrogen; Carlsbad, CA) according to the manufacturer's protocol.

2 μL cDNA reaction products (30 μL total) were amplified with forward and reverse primers: VEGFA (Hs00900055_m1, Applied Biosystems; Foster City, CA), ENO1 (Hs00361415_m1, Applied Biosystems), LDHA (Hs00855332_g1, Applied Biosystems), KLK3 (Hs02576345_m1, Applied Biosystems), FKBP5 (Hs01561006_m1, Applied Biosystems), TMPRSS2 (Hs01120965_m1, Applied Biosystems), HIF-1α (Hs00153153_m1, Applied Biosystems), and ACTB (Hs99999903_m1, Applied Biosystems). For each sample, 2 μl cDNA was mixed with 18 μL reaction mixture containing 1 μL forward and reverse primers, 7 μL water, and 10 μL Taqman Gene Expression Master Mix (Applied Biosystems) for a total volume of 20 μL. qPCR was

Molecular Pharmacology Fast Forward. Published on March 31, 2015 as DOI: 10.1124/mol.114.097477
This article has not been copyedited and formatted. The final version may differ from this version.

performed using an Applied Biosystems StepOnePlus Real-Time PCR system with StepOne Software. All qPCR reactions were run in triplicate. β-Actin (ACTB) was used as a reference housekeeping gene. Fold-change in RNA levels was calculated using the $\Delta\Delta C_t$ method (SABiosciences 2009 RT2 Profiler PCR Array System User Manual; Frederick, MD).

Enzyme-Linked Immunosorbent Assay (ELISA)

LNCaP cells were plated at a density of 10,000 cells per well in a 96-well dish in phenol red-free RPMI 1640 charcoal stripped media for 48 h at 37°C and then treated for 18 h at 37°C with combinations of DHT, chetomin, enzalutamide and hypoxic conditions (treatment with 150 μM $CoCl_2$). Conditioned media were collected and assayed with a VEGF ELISA (R&D systems; Minneapolis, MN).

Luciferase Reporter Assay

LNCaP cells were grown in 96-well plates in phenol red-free RPMI 1640 with 10% FBS and cells were transiently transfected with siRNA. After 48 h of siRNA treatment, cells were transiently transfected with reporter plasmids using Lipofectamine 2000 according to the manufacturer's instructions. Twenty-four hours after transfection, cells were then treated in phenol red-free, charcoal-stripped media containing combinations of DHT and enzalutamide under normoxia or hypoxia (150 μM $CoCl_2$) for 18 h. Transfection efficiency was normalized using pRL-TK (control reporter vector). Firefly and *Renilla* luciferase activities were determined using the Dual-Luciferase® Reporter Assay System (Promega). Firefly luciferase measurements were taken on a GloMax Multi+ Microplate

Molecular Pharmacology Fast Forward. Published on March 31, 2015 as DOI: 10.1124/mol.114.097477
This article has not been copyedited and formatted. The final version may differ from this version.

reader (Promega) and normalized using the *Renilla* luciferase measurements. All measurements were done in quadruplicate.

Statistical considerations

The Student's *t*-test was used for comparisons between treatment and: expression of gene transcripts, luciferase reporter assays, and ELISAs. Linear regression was used to test for the relationship between luciferase induction and increasing concentrations of HIF-1α inhibitors or DHT. One-way analysis of variance (ANOVA) followed by Dunnett's multiple comparisons test was performed to test for differences in treatments with percent cell count versus time. All comparisons were conducted using GraphPad Prism software (GraphPad Prism version 6.00, GraphPad Software, La Jolla CA). Significance was assigned to any observation in which $P \leq 0.05$.

Molecular Pharmacology Fast Forward. Published on March 31, 2015 as DOI: 10.1124/mol.114.097477
This article has not been copyedited and formatted. The final version may differ from this version.

RESULTS

DHT- and cobalt chloride-induced transcription of AR and HIF-1α target genes

To delineate the crosstalk between HIF-1α and AR pathways, prostate cancer hormone-sensitive LNCaP cells were treated with 1nM dihydrotestosterone (DHT) and 150 μM of the hypoxia mimetic cobalt chloride ($CoCl_2$) and assessed for the expression of androgen-responsive genes (*KLK3, FKBP5, TMPRSS2*) and hypoxia-induced genes (*VEGF, ENO1, LDHA*). While DHT increased the expression of the AR-regulated genes by ≥ 5.1-fold ($P<0.0001$; **Figure 1A**), $CoCl_2$ treatment alone reduced expression of all AR targets by ≤0.875-fold ($P\leq0.011$). The addition of $CoCl_2$ did not change DHT-induced transcription (*FKPB5* and *TMPRSS2*, $P\geq0.19$). $CoCl_2$-treatment increased the transcription of three HIF-1α targets by ≥1.8-fold ($P<0.0001$; **Figure 1B**), while DHT treatment alone under normoxia caused increased transcription of two HIF-1α targets, *VEGF* and *LDHA*, by ≥1.3-fold ($P\leq0.03$); *ENO1* expression was not affected ($P=0.55$). The addition of DHT either increased $CoCl_2$-induced transcription (*VEGF* 3.6-fold vs. 4.9 fold over untreated control, $P=0.021$) or did not change gene expression (*ENO1* and *LDHA*, $P\geq0.60$). Therefore, gene expression of all studied AR targets was repressed by hypoxia; conversely, specific HIF-1α target genes were induced by DHT-mediated AR signaling. This suggests that the crosstalk between the two pathways is complex and gene-specific; simultaneous treatment with both DHT and $CoCl_2$ typically minimized the effects of such crosstalk on transcription producing no synergistic effect.

Molecular Pharmacology Fast Forward. Published on March 31, 2015 as DOI: 10.1124/mol.114.097477
This article has not been copyedited and formatted. The final version may differ from this version.

Repression of AR-responsive gene transcription by enzalutamide and HIF-1α inhibition

We next ascertained whether repression of AR-signaling was potentiated by repression of HIF-1α signaling. LNCaP cells were exposed to the AR inhibitor, enzalutamide, in the presence or absence of chetomin, a known HIF-1α inhibitor that disrupts the binding of p300 to both HIF-1α and HIF-2α (Kung, Zabludoff et al. 2004). Without $CoCl_2$ stimulation, chetomin or enzalutamide mono-treatment similarly repressed transcription of *FKBP5* (5.1-fold vs. 1.1- and 1.0-fold respectively) and *TMPRSS2* (11.8-fold vs. 1.6- and 1.0-fold respectively) in the presence of DHT (see **Figure 2**). Chetomin was actually a better inhibitor of *KLK3* transcription than enzalutamide (38.2-fold vs. 1.8- and 4.2-fold respectively, (P<0.001). Co-treatment with chetomin and enzalutamide reduced transcription of all AR target genes to an even greater extent than either chetomin or enzalutamide alone (P≤0.012). During simultaneous DHT and $CoCl_2$ treatment, chetomin repressed the transcription of all AR targets to an even greater extent than enzalutamide (P≤0.0080) and co-treatment with chetomin and enzalutamide repressed transcription even further (P≤0.047). Similar results were observed in another hormone-sensitive prostate cancer 22Rv1 cell line (see **Supplementary Figure 1**).

While chetomin treatment resulted in suppression of AR target gene expression in LNCaPs, it counter-intuitively caused a greater dose-dependent increase in AR transcriptional activity (as determined by androgen-responsive luciferase reporter assay) than even DHT (see **Supplementary Figure 2A, B**). Shikonin, another HIF-1α inhibitor, also increased DHT-induced AR transactivation, albeit to a lesser extent in the concentrations tested (**Supplementary Figure 2C**). A natural product-based screen using a HIF-1α-p300 assay developed in our laboratory led to the identification of shikonin

Molecular Pharmacology Fast Forward. Published on March 31, 2015 as DOI: 10.1124/mol.114.097477
This article has not been copyedited and formatted. The final version may differ from this version.

being able to reduce the tight interaction between a HIF-1α fragment and the CH1 domain of p300 (W.D. Figg, unpublished observations). This effect is likely due to the pleiotropic effects of chetomin and shikonin, which inhibit transcriptional complexes containing the rather promiscuous p300.

Therefore, we tested the hypothesis that specific HIF-1α knockdown potentiates the AR-repressive effect of enzalutamide. LNCaP cells transfected with HIF-1α siRNA specifically knocked down the mRNA expression of both HIF-1α (1.0- vs. 0.38-fold and 1.9- vs. 0.22-fold, $P \leq 0.001$; **Figure 3A**) and VEGFA (during CoCl2 treatment, 3.6- vs. 2.0-fold, $P=0.019$; **Figure 3B**) as well as other transcriptional targets of HIF-1α (*ENO1*, *LDHA*, see **Supplementary Figure 3**), indicating the specificity and effectiveness of the HIF-1α siRNA tested. We next assessed the effect of HIF-1α siRNA on DHT- and $CoCl_2$ -enhanced AR transactivation in the presence of enzalutamide. As expected, enzalutamide decreased AR transactivation ($P \leq 0.0071$; **Figure 3C**). HIF-1α siRNA had similar effects as chetomin in reducing DHT- and $CoCl_2$ -enhanced AR transactivation ($P \leq 0.034$), and had a synergistic AR-repressive effect in the presence of enzalutamide ($P \leq 0.010$; **Figure 3C**). Similar observations were noted in 22Rv1 cells with the combination of HIF-1α siRNA and enzalutamide being more effective in reducing AR transactivation than either treatment alone ($P<0.001$; **Figure 3D**). The similarity between the results presented in **Figures 2** and **3** suggest that chetomin's HIF/p300 repressive effect on specific gene expression in prostate cancer cells supersedes its ability to promote ARE-mediated transactivation on the global transcription machinery.

Molecular Pharmacology Fast Forward. Published on March 31, 2015 as DOI: 10.1124/mol.114.097477
This article has not been copyedited and formatted. The final version may differ from this version.

Repression of hypoxia-mediated gene expression by enzalutamide and HIF-1α inhibition

We next determined the effect of AR and HIF-1α inhibition on hypoxia-induced gene expression. LNCaP cells were cultured in the presence or absence of DHT (1 nM) under normoxic or hypoxic (150 μM $CoCl_2$) conditions for 18 h, and treated with 1 μM enzalutamide or 100 nM chetomin or both drugs followed by qPCR analysis. Under CoCl2 treatment, chetomin significantly reduced all HIF-1α targets to near, or below basal levels (P<0.001) (**Figure 4A-C**). During $CoCl_2$ and DHT co-treatment, enzalutamide decreased VEGF transcription (3.0- vs. 4.9-fold; P<0.001; **Figure 4A**), while other HIF targets were not affected (P>0.25; see **Figure 4B, C**). We further measured VEGF at the protein level in the conditioned medium by ELISA. Enzalutamide treatment resulted in reduced VEGF release in the medium, and the inhibitory effect was synergistic with HIF-1α silencing using HIF-1α siRNA (**Figure 4D, E**, P<0.0001). Similar results were obtained in the 22Rv1 prostate cancer cell line (**Figure 4F**).

HIF-1α knockdown synergistically enhances enzalutamide activity

Given the significant crosstalk between the HIF and AR pathways, we determined the biological implications of this interaction by assessing the effects of AR inhibition and HIF-1α inhibition on the growth of LNCaP cells during $CoCl_2$ and DHT treatment. As shown in **Figure 5A**, enzalutamide inhibited LNCaP cell growth in cells transfected with scrambled siRNA. Similarly, HIF-1α siRNA also reduced cell growth when treated with $CoCl_2$. Simultaneous treatment with HIF-1α siRNA synergistically enhanced the inhibitory effect of enzalutamide on LNCaP cell viability. We evaluated the effect of HIF-1α inhibition on the enzalutamide-resistant resistant 22Rv1 prostate cancer cell line,

and found that the treatment combination was also effective at reducing cell growth of the enzalutamide-resistant 22Rv1 prostate cancer cell line, albeit at a delayed response (48 h) compared to LNCaPs (24 h) (**Figure 5B**). In addition, the combination approach also resulted in HIF-1α inhibition synergistically enhancing enzalutamide-induced apoptosis, as shown by cleaved poly-ADP-ribose polymerase (PARP) (**Figure 5C**).

Molecular Pharmacology Fast Forward. Published on March 31, 2015 as DOI: 10.1124/mol.114.097477
This article has not been copyedited and formatted. The final version may differ from this version.

DISCUSSION

Prostate cancer is largely driven by aberrant androgen signaling and tumor hypoxia. Thus, inhibiting hypoxia may be key in increasing the efficacy of AR-targeted therapy. Here, we proposed that inhibiting HIF-1α potentiates enzulatamide treatment, thereby demonstrating that simultaneously targeting of both HIF-1α and AR pathways is an effective treatment option for CRPC.

Given the conflicting literature reports concerning AR activity under hypoxic conditions in different experimental systems, we first examined the crosstalk between HIF-1α and AR pathways by evaluating the effect of androgen and hypoxia on multiple AR- and HIF-1α targets. We found that hypoxia repressed all AR target gene expression; this is consistent with findings from Ghafar et al (2003), which showed that hypoxia-response (up to 24hours) acutely decreased expression of prostate-specific antigen protein levels. Conversely, specific HIF-1α target genes were induced by liganded AR activation. Previous studies have found that hypoxia activated AR only in the presence of androgen (Horii, Suzuki et al. 2007; Park, Kim et al., 2012). Others showed unliganded AR transactivation in cells exposed to hypoxia (Khandrika, Lieberman, et al. 2009) or that hypoxia only activated the AR at low androgen concentrations mimicking the castration-resistant stage (Mitani, Yamaji et al., 2011) involving AR, HIF-1α, and β-catenin forming a ternary complex on AREs (Mitani, Harada et al., 2012). Similarly, the effect of AR activation on HIF-mediated transcription was either induction (Mabjeesh, Willard et al., 2003; Horii, Suzuki et al., 2007) or no synergistic effect (Park, Kim et al., 2012). Our findings in the current study suggest that the crosstalk between the two pathways is complexly regulated in a gene-specific manner; however, the simultaneous

Molecular Pharmacology Fast Forward. Published on March 31, 2015 as DOI: 10.1124/mol.114.097477
This article has not been copyedited and formatted. The final version may differ from this version.

treatment with both DHT and $CoCl_2$ typically minimized the effects of such crosstalk on gene transcription.

We determined the effect of enzalutamide and HIF-1α inhibition on mediating AR-responsive and hypoxia-induced gene expression. We found that HIF-1α repression (using either chetomin or HIF-1α siRNA) potentiated the AR-repressive effect of enzalutamide; however, the combination of enzalutamide and HIF-1α inhibition resulted in specific repression of hypoxia-induced VEGF expression. Simultaneous treatment with HIF-1α siRNA synergistically enhanced the inhibitory effect of enzalutamide on LNCaP cell viability through increased apoptosis. Surprisingly, this treatment combination was also effective at reducing the growth rate of the enzalutamide-resistant 22Rv1 prostate cancer cell line, suggesting that HIF-1α inhibition can restore sensitivity to enzalutamide-resistant cells. Li et al. (Li, Chan et al., 2013) demonstrated that C-terminally truncated, constitutively active AR splice variants (AR-Vs) lacking the ligand binding domain limit the efficacy of enzalutamide since only knockdown of AR-Vs, not of full-length AR, was able to restore the ability of enzalutamide to inhibit cell proliferation of AR/AR-V coexpressing 22Rv1 prostate cancer cells. Exploration of novel avenues to potentiate anti-AR therapy is needed to overcome the effects of AR/AR-V signaling or enzalutamide resistance. Potential pathways include inhibition of cellular signaling networks based on targeting compensatory survival pathways associated with relief of feedback inhibition. Indeed recent studies have proposed that combined targeting of the PI3K/AKT and AR pathways (Carver, Chapinski et al., 2011; Toren, Kim, et al. 2014) suggest a possible approach to overcome enzalutamide resistance, providing support for further evaluation in the clinic.

Molecular Pharmacology Fast Forward. Published on March 31, 2015 as DOI: 10.1124/mol.114.097477
This article has not been copyedited and formatted. The final version may differ from this version.

In the present study, we provide a strong rationale for the combined targeting of the HIF-1α and AR pathways. Enzalutamide's effect on HIF-1α-regulated gene expression is specifically targeted to VEGF, thus making VEGF a potential biomarker for assessing enzalutamide response; studies are underway to evaluate this effect in clinical treatment samples. Our results are consistent with a gene expression profiling study in LNCaP cells that indicate enzalutamide opposing agonist-induced changes in genes involved in processes such as angiogenesis (Guerrero, Alfaro et al., 2013). Moreover, a recent clinical study found that nonspecific HIF-1α inhibitors (digoxin, metformin, angiotensin-2 receptor blockers) appear to increase progression-free survival and reduce the risk of developing CRPC and metastases in patients on continuous ADT (Ranasinghe, Sengupta et al., 2014). Whether combining nonspecific HIF-1α inhibitors with existing second generation antiandrogens might produce an added survival benefit remains to be investigated. Our laboratory is involved in developing several specific small molecule HIF-1α inhibitors, and ongoing preclinical studies evaluating the combination of these HIF-1α inhibitors with enzalutamide are currently underway. Taken together, dual targeting of the AR and HIF-1 axis represents an attractive approach for CRPC treatment with HIF-1α inhibition as a possible mechanism for overcoming enzalutamide resistance and potentiating anti-AR therapy.

Molecular Pharmacology Fast Forward. Published on March 31, 2015 as DOI: 10.1124/mol.114.097477
This article has not been copyedited and formatted. The final version may differ from this version.

AUTHORSHIP CONTRIBUTIONS

Participated in research design: E.V.F., K.M.R., S.M.T., T.M.S., D.K.P, C.H.C., W.D.F.
Conducted experiments: E.V.F., K.M.R., A.M.L., S.M.T.
Contributed new reagents or analytic tools:
Performed data analysis: E.V.F., K.M.R., A.M.L., S.M.T., T.M.S., D.K.P, C.H.C., W.D.F.
Wrote or contributed to the writing of the manuscript: E.V.F., K.M.R., A.M.L., S.M.T., T.M.S., D.K.P, C.H.C., W.D.F.

Molecular Pharmacology Fast Forward. Published on March 31, 2015 as DOI: 10.1124/mol.114.097477
This article has not been copyedited and formatted. The final version may differ from this version.

REFERENCES

Carver, B. S., C. Chapinski, J. Wongvipat, H. Hieronymus, Y. Chen, S. Chandarlapaty, V. K. Arora, C. Le, J. Koutcher, H. Scher, P. T. Scardino, N. Rosen and C. L. Sawyers (2011). "Reciprocal feedback regulation of PI3K and androgen receptor signaling in PTEN-deficient prostate cancer." *Cancer Cell* **19**(5): 575-586.

Chen, C. D., D. S. Welsbie, C. Tran, S. H. Baek, R. Chen, R. Vessella, M. G. Rosenfeld and C. L. Sawyers (2004). "Molecular determinants of resistance to antiandrogen therapy." *Nat Med* **10**(1): 33-39.

Debes, J. D. and D. J. Tindall (2004). "Mechanisms of androgen-refractory prostate cancer." *N Engl J Med* **351**(15): 1488-1490.

Ghafar, M.A., A.G. Anastasiadis, M.W. Chen, M. Burchardt, L. E. Olsson, H. Xie, M.C. Benson, and R. Buttyan (2003). " AcuteHypoxia Increases the Aggressive Characteristics and Survival Properties of Prostate Cancer Cells." *The Prostate* **54** (1): 58-67.

Greer, S. N., J. L. Metcalf, Y. Wang and M. Ohh (2012). "The updated biology of hypoxia-inducible factor." *EMBO J* **31**(11): 2448-2460.

Guerrero, J., I. E. Alfaro, F. Gomez, A. A. Protter and S. Bernales (2013). "Enzalutamide, an androgen receptor signaling inhibitor, induces tumor regression in a mouse model of castration-resistant prostate cancer." *Prostate* **73**(12): 1291-1305.

Halin, S., P. Hammarsten, P. Wikstrom and A. Bergh (2007). "Androgen-insensitive prostate cancer cells transiently respond to castration treatment when growing in an androgen-dependent prostate environment." *Prostate* **67**(4): 370-377.

Horii, K., Y. Suzuki, Y. Kondo, M. Akimoto, T. Nishimura, Y. Yamabe, M. Sakaue, T. Sano, T. Kitagawa, S. Himeno, N. Imura and S. Hara (2007). "Androgen-dependent gene expression of prostate-specific antigen is enhanced synergistically by hypoxia in human prostate cancer cells." *Mol Cancer Res* **5**(4): 383-391.

Khandrika, L., R. Lieberman, S. Koul, B. Kumar, P. Maroni, R. Chandhoke, R. B. Meacham and H. K. Koul (2009). "Hypoxia-associated p38 mitogen-activated protein kinase-mediated androgen receptor activation and increased HIF-1alpha levels contribute to emergence of an aggressive phenotype in prostate cancer." *Oncogene* **28**(9): 1248-1260.

Kung, A. L., S. D. Zabludoff, D. S. France, S. J. Freedman, E. A. Tanner, A. Vieira, S. Cornell-Kennon, J. Lee, B. Wang, J. Wang, K. Memmert, H. U. Naegeli, F. Petersen, M. J. Eck, K. W. Bair, A. W. Wood and D. M. Livingston (2004). "Small molecule blockade of

transcriptional coactivation of the hypoxia-inducible factor pathway." *Cancer Cell* **6**(1): 33-43.

Li, Y., S. C. Chan, L. J. Brand, T. H. Hwang, K. A. Silverstein and S. M. Dehm (2013). "Androgen receptor splice variants mediate enzalutamide resistance in castration-resistant prostate cancer cell lines." *Cancer Res* **73**(2): 483-489.

Mabjeesh, N. J., M. T. Willard, C. E. Frederickson, H. Zhong and J. W. Simons (2003). "Androgens stimulate hypoxia-inducible factor 1 activation via autocrine loop of tyrosine kinase receptor/phosphatidylinositol 3'-kinase/protein kinase B in prostate cancer cells." *Clin Cancer Res* **9**(7): 2416-2425.

Mitani, T., N. Harada, Y. Nakano, H. Inui and R. Yamaji (2012). "Coordinated action of hypoxia-inducible factor-1alpha and beta-catenin in androgen receptor signaling." *J Biol Chem* **287**(40): 33594-33606.

Mitani, T., R. Yamaji, Y. Higashimura, N. Harada, Y. Nakano and H. Inui (2011). "Hypoxia enhances transcriptional activity of androgen receptor through hypoxia-inducible factor-1alpha in a low androgen environment." *J Steroid Biochem Mol Biol* **123**(1-2): 58-64.

Nelson, W. G. and S. Yegnasubramanian (2013). "Resistance emerges to second-generation antiandrogens in prostate cancer." *Cancer Discov* **3**(9): 971-974.

Park, C., Y. Kim, M. Shim and Y. Lee (2012). "Hypoxia enhances ligand-occupied androgen receptor activity." *Biochem Biophys Res Commun* **418**(2): 319-323.

Pienta, K. J. and D. Bradley (2006). "Mechanisms underlying the development of androgen-independent prostate cancer." *Clin Cancer Res* **12**(6): 1665-1671.

Ranasinghe, W. K., S. Sengupta, S. Williams, M. Chang, A. Shulkes, D. M. Bolton, G. Baldwin and O. Patel (2014). "The effects of nonspecific HIF1alpha inhibitors on development of castrate resistance and metastases in prostate cancer." *Cancer Med* **3**(2): 245-251.

Scher, H. I. and C. L. Sawyers (2005). "Biology of progressive, castration-resistant prostate cancer: directed therapies targeting the androgen-receptor signaling axis." *J Clin Oncol* **23**(32): 8253-8261.

Semenza, G. L. (2010). "Defining the role of hypoxia-inducible factor 1 in cancer biology and therapeutics." *Oncogene* **29**(5): 625-634.

Semenza, G. L. (2012). "Hypoxia-inducible factors in physiology and medicine." *Cell* **148**(3): 399-408.

Shabsigh, A., M. A. Ghafar, A. de la Taille, M. Burchardt, S. A. Kaplan, A. G. Anastasiadis and R. Buttyan (2001). "Biomarker analysis demonstrates a hypoxic environment in the castrated rat ventral prostate gland." *J Cell Biochem* **81**(3): 437-444.

Sharifi, N., E. M. Hurt, S. B. Thomas and W. L. Farrar (2008). "Effects of manganese superoxide dismutase silencing on androgen receptor function and gene regulation: implications for castration-resistant prostate cancer." *Clin Cancer Res* **14**(19): 6073-6080.

Stewart, G. D., J. A. Ross, D. B. McLaren, C. C. Parker, F. K. Habib and A. C. Riddick (2010). "The relevance of a hypoxic tumour microenvironment in prostate cancer." *BJU Int* **105**(1): 8-13.

Toren, P., S. Kim, T. Cordonnier, C. Crafter, B. R. Davies, L. Fazli, M. E. Gleave and A. Zoubeidi (2014). "Combination AZD5363 with Enzalutamide Significantly Delays Enzalutamide-resistant Prostate Cancer in Preclinical Models." *Eur Urol.*

Tran, C., S. Ouk, N. J. Clegg, Y. Chen, P. A. Watson, V. Arora, J. Wongvipat, P. M. Smith-Jones, D. Yoo, A. Kwon, T. Wasielewska, D. Welsbie, C. D. Chen, C. S. Higano, T. M. Beer, D. T. Hung, H. I. Scher, M. E. Jung and C. L. Sawyers (2009). "Development of a second-generation antiandrogen for treatment of advanced prostate cancer." *Science* **324**(5928): 787-790.

FOOTNOTES

This research was supported in part by the Intramural Research Program of the National Institutes of Health, National Cancer Institute, Center for Cancer Research.

The content of this publication does not necessarily reflect the views or policies of the Department of Health and Human Services, nor does mention of trade names, commercial products, or organization imply endorsement by the U.S. Government.

E.V.F. and K.M.R. contributed equally to this work.

Molecular Pharmacology Fast Forward. Published on March 31, 2015 as DOI: 10.1124/mol.114.097477
This article has not been copyedited and formatted. The final version may differ from this version.

FIGURES LEGENDS

Figure 1. Effect of DHT and $CoCl_2$ on AR-dependent and hypoxia-inducible gene transcription. (A) LNCaP cells were cultured in the presence or absence of DHT (1 nM) under normoxic or hypoxic (150 μM $CoCl_2$) conditions for 18 h. Total RNA was extracted and qPCR analyses were performed for (A) AR-dependent target genes (KLK3, FKBP5, TMPRSS2); (B) Hypoxia-dependent target genes (VEGF, ENO1, LDHA) and β-actin mRNA expression. Relative mRNA levels of each target gene expression are normalized by β-actin expression, and the results are indicated as fold change from those in the absence of DHT in normoxia. The result is representative of three independent experiments. **P*<0.05, ***P*<0.01, ****P*<0.001 on Figure.

Figure 2. Effect of the AR antagonist, enzalutamide, and the HIF-1α inhibitor, chetomin, on AR-dependent gene transcription. LNCaP cells were cultured in the presence or absence of DHT (1 nM) under normoxic or hypoxic (150 μM $CoCl_2$) conditions for 18 h. Cells were treated with 1 μM enzalutamide or 100 nM chetomin. Total RNA was extracted and qPCR analyses were performed for AR-dependent target genes (KLK3, FKBP5, TMPRSS2) and β-actin mRNA expression. Relative mRNA levels of each target gene expression are normalized by β-actin expression, and the results are indicated as fold change from those in the absence of DHT in normoxia. The result is representative of three independent experiments. (A) *KLK3*, (B) FKBP5, (C) TMPRSS2. **P*<0.05, ***P*<0.01, ****P*<0.001 on Figure.

Figure 3. Effects of HIF siRNA and enzalutamide on AR transcriptional activation.

Molecular Pharmacology Fast Forward. Published on March 31, 2015 as DOI: 10.1124/mol.114.097477
This article has not been copyedited and formatted. The final version may differ from this version.

LNCaP cells were treated with 20 nM HIF-1α siRNA (siHIF-1α) or control siRNA (siControl) for 48 h. Cells were incubated in normoxia (N) or $CoCl_2$ for an additional 18 h. HIF-1α siRNA repressed (A) HIF and (B) VEGF transcripts. (C) After siRNA treatment, cells were transfected with pARE-Luc and pRL-TK for 24 h followed by treatment with enzalutamide in the presence and absence of 1 nM DHT in normoxia or hypoxia for an additional 18 h. Luciferase activities were determined, and data are expressed as means ± SEM (n = 3). HIF-1α siRNA and enzalutamide repressed ARE luciferase activation ($P \leq 0.034$), whereas combined HIF-1α siRNA and enzalutamide treatment was more effective than either treatment alone ($P \leq 0.010$). (D) HIF siRNA and enzalutamide repressed ARE-luc activation in 22Rv1 cells ($P < 0.001$), and enzalutamide treatment was more effective than either treatment alone ($P < 0.001$). *$P < 0.05$, **$P \leq 0.01$, ***$P < 0.001$ on Figure.

Figure 4. Effect of enzalutamide and HIF inhibition on hypoxia-induced gene expression. (A–C) LNCaP cells were cultured in the presence or absence of DHT (1 nM) under normoxic or hypoxic (150 μM $CoCl_2$) conditions for 18 h. Cells were treated with 1 μM enzalutamide or 100 nM chetomin. Total RNA was extracted and mRNA levels were analyzed by qPCR for hypoxia-dependent target genes (VEGF, ENO1, LDH1) and β-actin as an internal standard. Relative mRNA levels of each target gene expression are normalized by β-actin expression, and the results are indicated as fold change from those in the absence of DHT in normoxia. The result is representative of three independent experiments. (A) VEGF; (B) ENO1; (C) LDHA. (D–F) Enzalutamide inhibits VEGF secretion. (D) LNCaP cells treated with 1 μM enzalutamide in the presence or absence of

1 nM DHT under normoxic or hypoxic conditions for 18 h. Conditioned media were collected and VEGF protein levels were measured by ELISA. The concentrations of VEGF (picogram per milliliter) per the total number of cells in each well were calculated, and results are expressed as the fold induction of VEGF secretion compared to untreated controls. Each point represents the mean ± SEM of three different determinations each performed in triplicate. (E) LNCaP cells were treated with 20 nM HIF-1α siRNA (siHIF-1α) or control siRNA (siControl) for 48 h followed by treatment as above. (F) 22Rv1 cells were treated with 20 nM HIF-1α siRNA (siHIF-1α) or control siRNA (siControl) for 24 h followed by treatment as above.

Figure 5. Effect of HIF-1α siRNA and enzalutamide on (A) LNCaP cell growth over 72 h and (B) 22Rv1 cell growth over 120 h (**P*<0.05, ***P*≤0.01, ****P*<0.001). Cells were treated with HIF-1α siRNA or control siRNA for 48 h followed by 1 μM enzalutamide in the presence of 150 μM $CoCl_2$ and 1 nM DHT**.** Cell viability was determined using the Cell Counting-Kit 8 cell viability assay at the indicated time points. (C) Effect of HIF-1α siRNA and enzalutamide on cleavage of poly-ADP-ribose polymerase (PARP). Cells were treated as above, and whole cell lysates were analyzed by Western blot analysis.

Figure 1 (A&B)

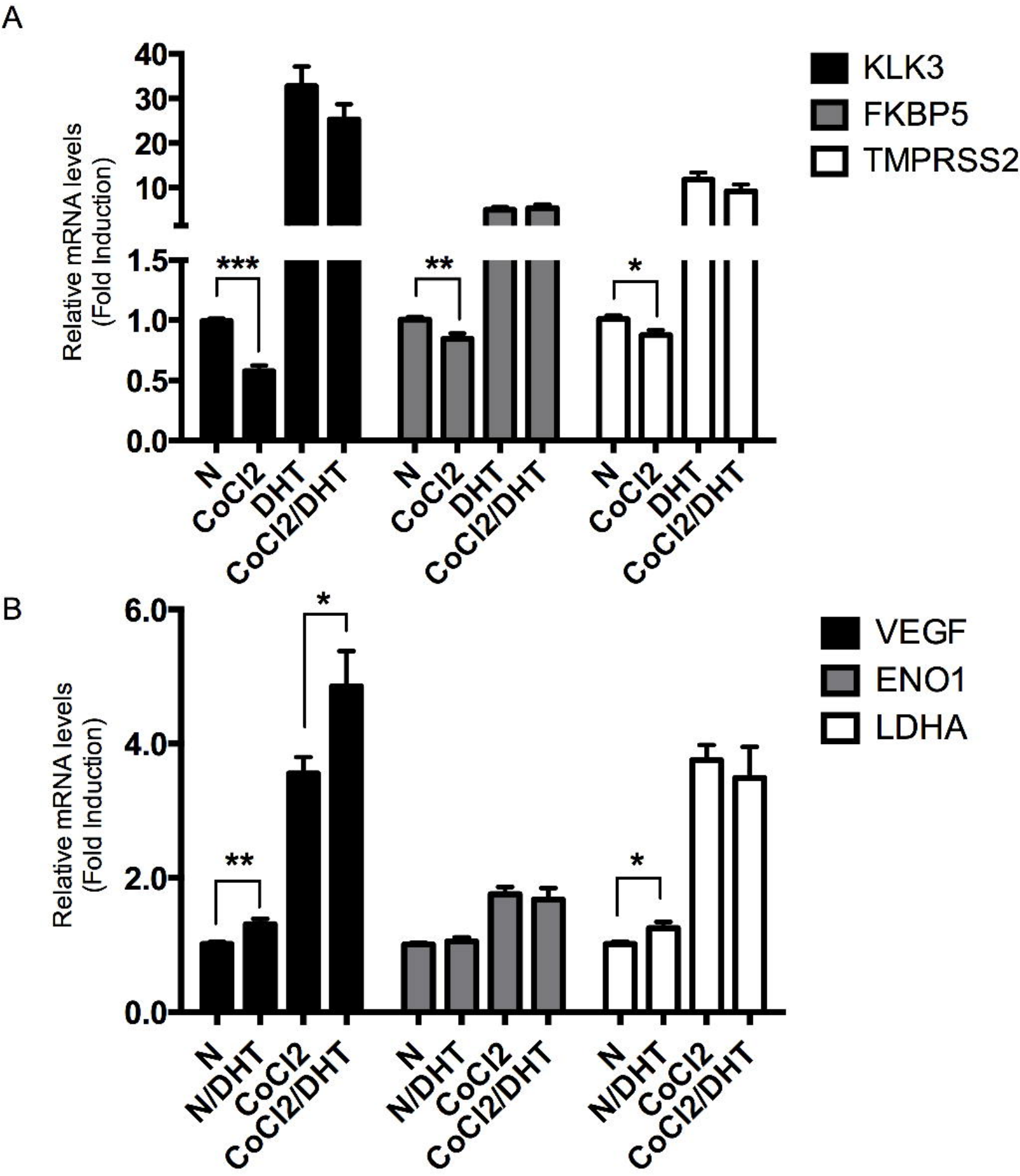
A
Relative mRNA levels
(Fold Induction)
40
30
20
10
1.5
1.0
0.5
0.0
***
**
*
KLK3
FKBP5
TMPRSS2
N
CoCl2
DHT
CoCl2/DHT
B
Relative mRNA levels
(Fold Induction)
6.0
4.0
2.0
0.0
**
*
*
VEGF
ENO1
LDHA
N
N/DHT
CoCl2
CoCl2/DHT

Figure 2 (A-C)

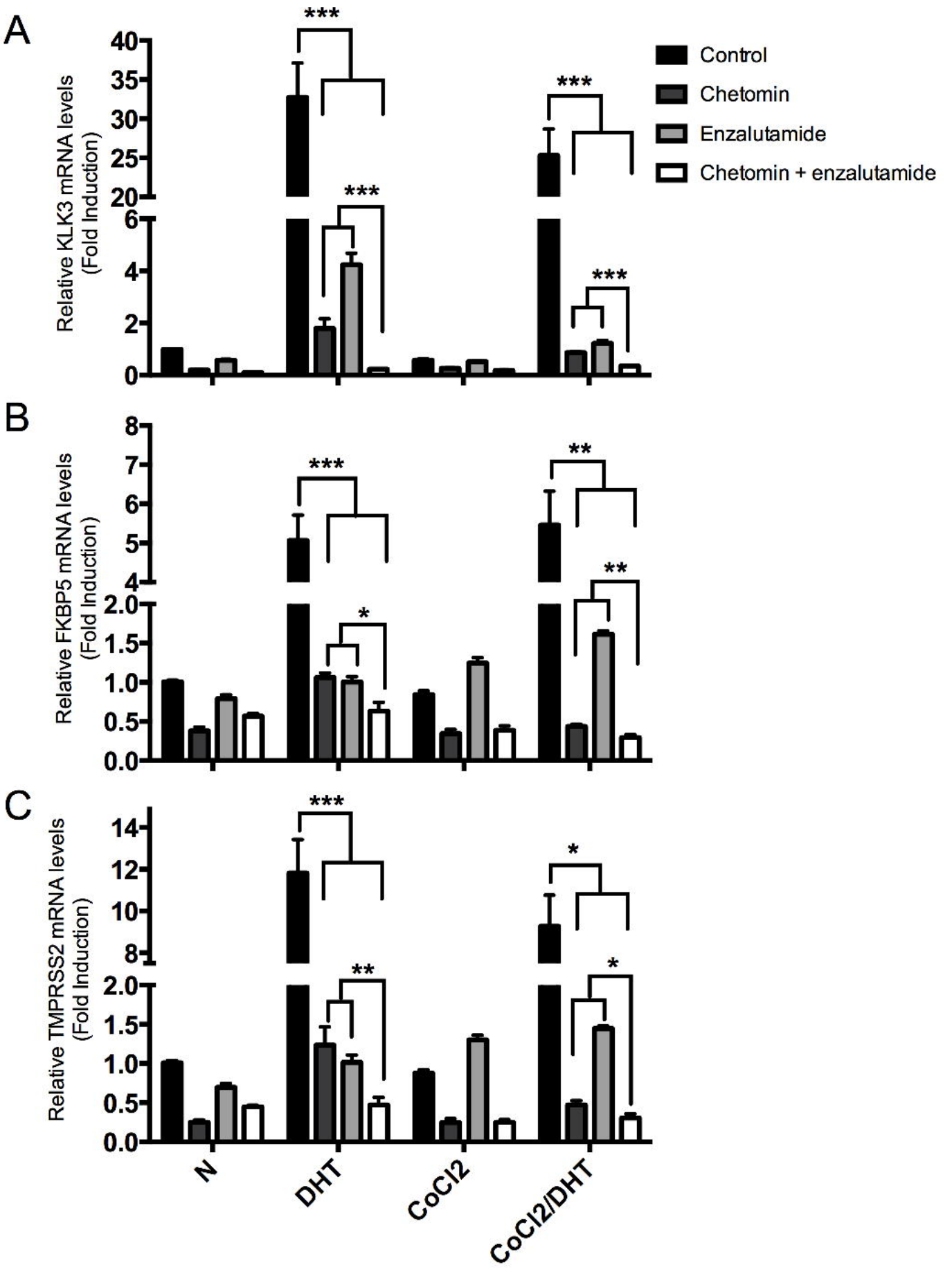
A
B
C
Relative KLK3 mRNA levels (Fold Induction)
Relative FKBP5 mRNA levels (Fold Induction)
Relative TMPRSS2 mRNA levels (Fold Induction)
Control
Chetomin
Enzalutamide
Chetomin + enzalutamide
N
DHT
CoCl2
CoCl2/DHT

Figure 3

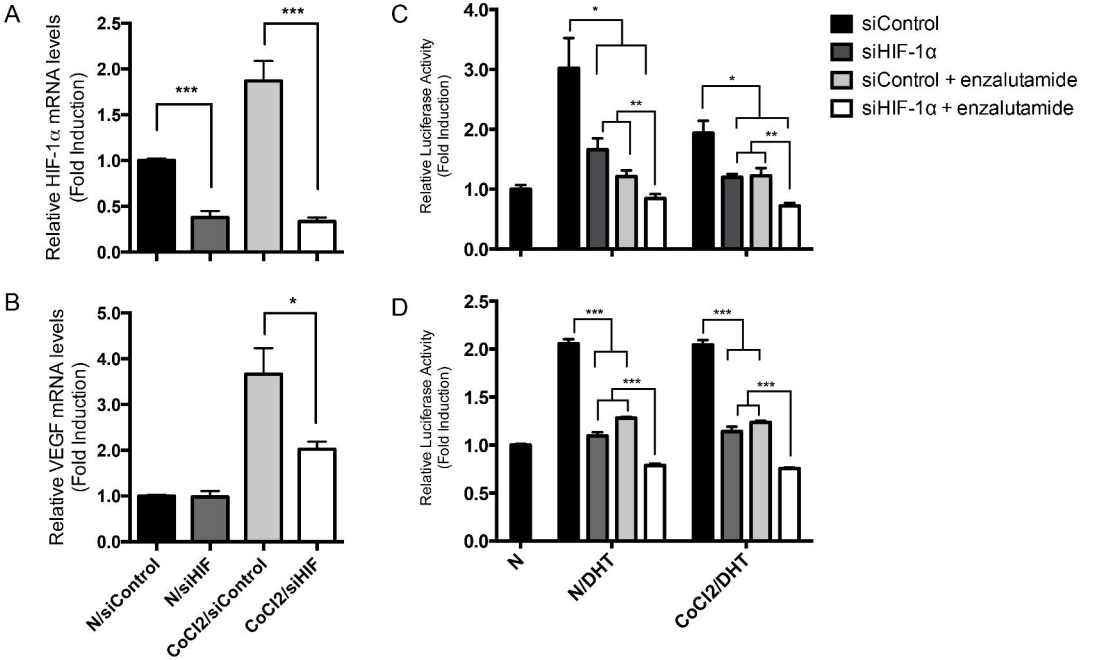
A
Relative HIF-1α mRNA levels (Fold Induction)
2.5
2.0
1.5
1.0
0.5
0.0
***
***
B
Relative VEGF mRNA levels (Fold Induction)
5.0
4.0
3.0
2.0
1.0
0.0
*
N/siControl
N/siHIF
CoCl2/siControl
CoCl2/siHIF
C
Relative Luciferase Activity (Fold Induction)
4.0
3.0
2.0
1.0
0.0
*
**
*
**
siControl
siHIF-1α
siControl + enzalutamide
siHIF-1α + enzalutamide
D
Relative Luciferase Activity (Fold Induction)
2.5
2.0
1.5
1.0
0.5
0.0
***
***
***
***
N
N/DHT
CoCl2/DHT

Figure 4 (A-C)

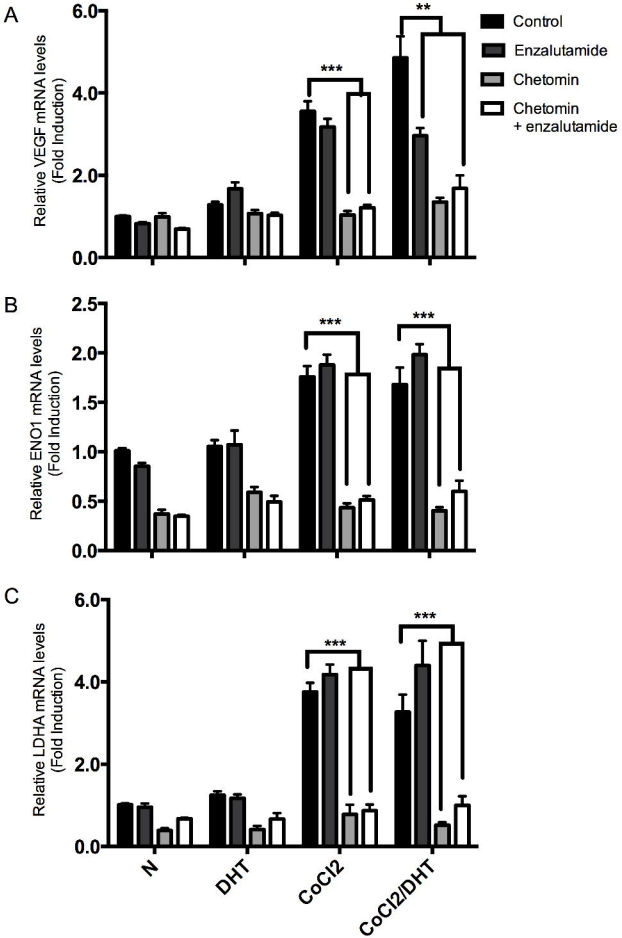

Figure 4 (D-F)

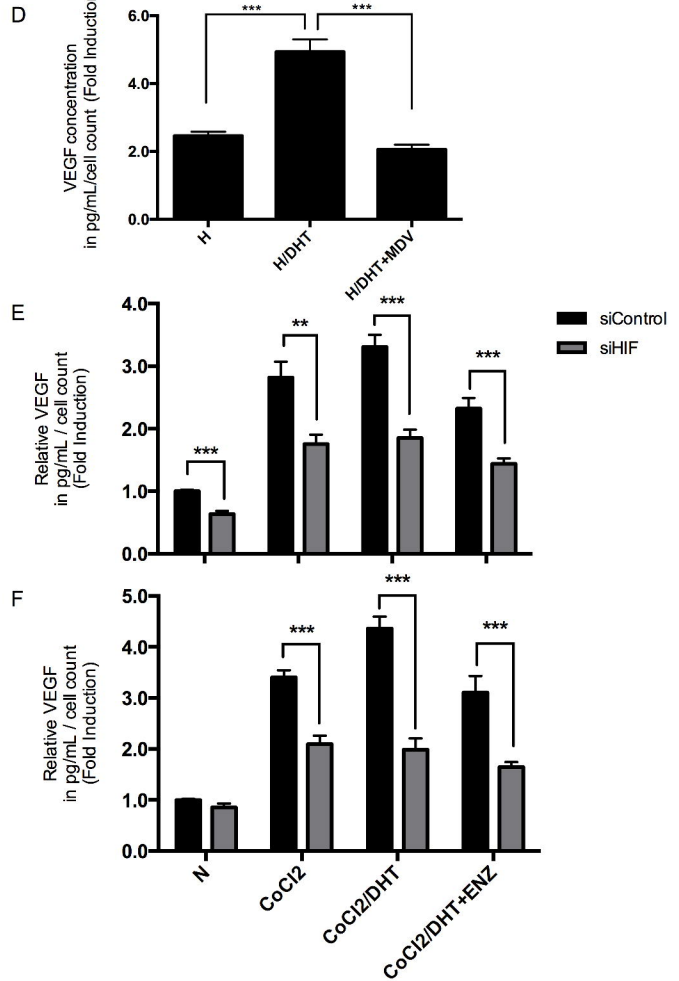

Figure 5 (A-C)

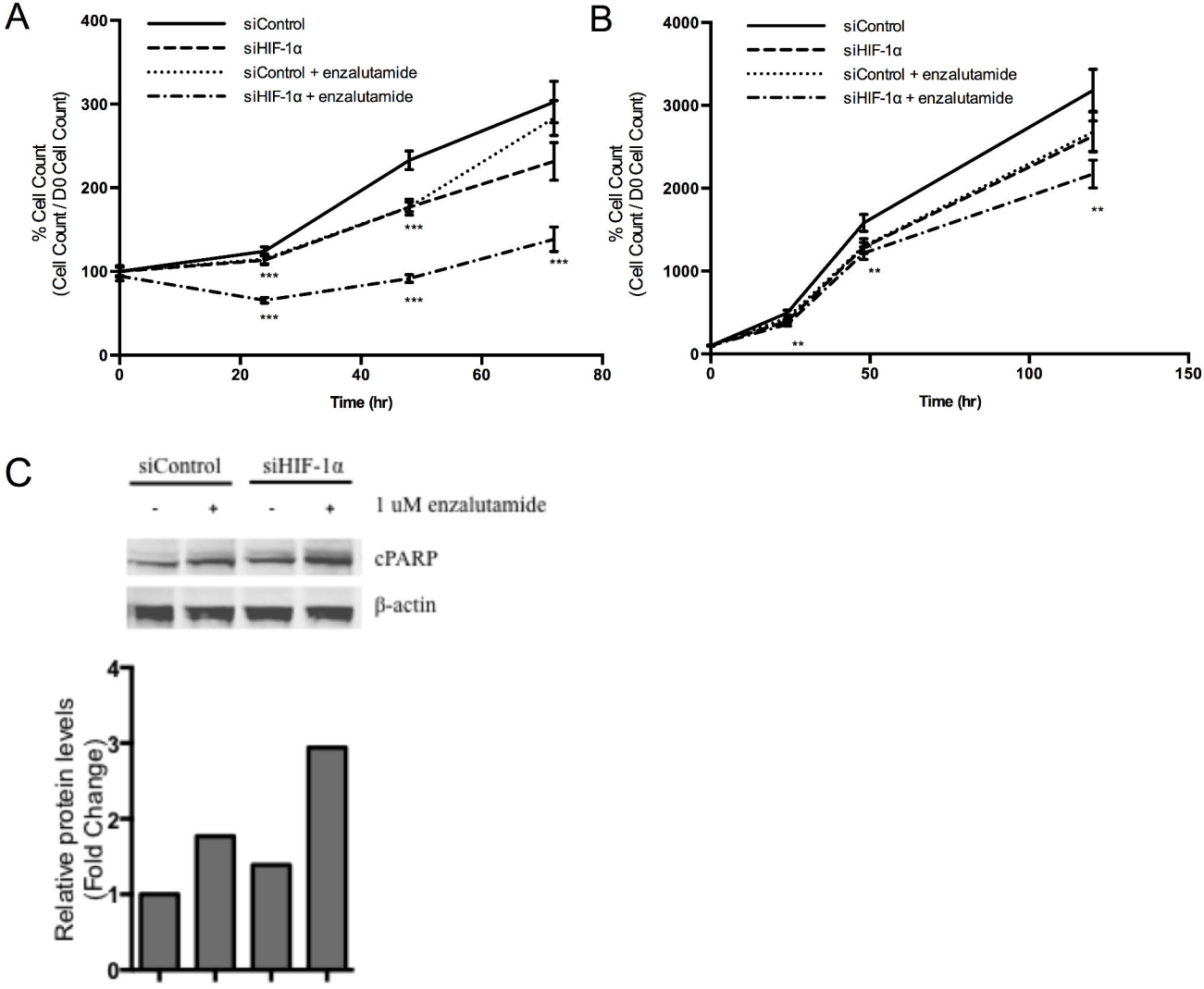
A
siControl
siHIF-1α
siControl + enzalutamide
siHIF-1α + enzalutamide
% Cell Count
(Cell Count / D0 Cell Count)
Time (hr)
B
C
siControl
siHIF-1α
1 uM enzalutamide
cPARP
β-actin
Relative protein levels
(Fold Change)